Mon. Not. R. Astron. Soc. **277**, 1435–1442 (1995)

Polarized radio filaments in the Vela X supernova remnant

D. K. Milne

Australia Telescope National Facility, CSIRO, PO Box 76 Epping, NSW 2121, Australia

Accepted 1995 July 24. Received 1995 July 24; in original form 1995 May 16

ABSTRACT

The radio-bright Vela X component of the Vela supernova remnant (SNR) was mapped in total intensity and in polarization at 8.4 GHz with 3-arcmin resolution. Prominent filamentary structure (unrelated to the optical filaments) is seen in the polarization image and to a lesser extent in total intensity. The filaments are highly polarized, with magnetic fields directed along the filaments. They have moderate Faraday rotation (mean RM ~ 44 rad m^{-2}) and little depolarization. Comparison with data at 5 and 2.7 GHz suggests that the overall spectral index is typical of a SNR and relatively uniform throughout the region.

Key words: magnetic fields – polarization – ISM: individual: Vela SNR – supernova remnants – radio continuum: ISM.

1 INTRODUCTION

The Vela supernova remnant (SNR) is most readily seen in the UV mosaic of Miller (1973) as a well-defined, near-circular nebula, 5° in diameter, with a number of filamentary shells mainly in the north-west. Radio maps at 408, 635, 1410 and 2650 MHz (Milne 1968) and 2700 MHz (Day, Caswell & Cooke 1972) show a low-level source of similar extent to the UV image, but with the brightest radio emission localized in the south-west quadrant. The pulsar 0833−45 is located near the inner (northern) edge of this radio-bright region, known as Vela X. There has been some controversy as to whether Vela X is part of the larger Vela SNR or whether it is a separate pulsar-driven remnant (a plerion) and not associated with the extended region (see Milne & Manchester 1986; Dwarakanath 1991).

In X-rays, the *Einstein* image of the Vela SNR (Kahn et al. 1985) appears brightest in the north-west and south-east quadrants, with well-defined edges in these directions. In the south the *Einstein* data are incomplete, and Kahn et al. thought it likely that the X-ray emission extended as much as 1° further than the radio and optical emission in that direction, a conclusion confirmed recently by the *ROSAT* observations (Aschenbach, Egger & Trümper 1995). In fact, the *ROSAT* image shows faint X-ray emission well to the west and south, and clearly implies that the pulsar is very close to the centre of an 8°.3-diameter, near-circular X-ray nebula, a nebula much larger than implied from the observed radio and optical features. More recently, Markwardt & Ögelman (1995) have demonstrated from the *ROSAT* data that an X-ray jet extends south for 45 arcmin from the pulsar position.

Because of the very large angular extent of the Vela SNR, high-resolution, radio-synthesis observations have not yet been undertaken and, above 2700 MHz, only the Vela X component has been mapped (at 5 GHz; Milne 1980, hereafter Paper I). Here I present maps of Vela X in total intensity and polarization at 8.4 GHz, at a somewhat higher frequency and resolution than used previously.

2 OBSERVATIONS

These observations were made in 1992 March with the Parkes 64-m radio telescope at 8.4 GHz. The dual-channel FET receiver accepts right- and left-hand circular polarization from the feed horn, and these are then converted to linear Stokes parameters Q and U in the correlation polarimeter. A linearly polarized noise signal transmitted from the telescope vertex, together with the sources 3C 138 ($I = 2.4$ Jy, $P = 10.7$ per cent at 173° PA) and Hydra A ($I = 8.1$ Jy), were used for calibration. Flux densities and polarization parameters for the calibration sources were taken from the Parkes Catalogue (Wright & Otrupcek 1990) and the compilation of Tabara & Inoue (1980). The system temperature was ~ 70 K, the bandwidth 500 MHz and the beamwidth 3 arcmin.

The field was scanned in declination and right ascension and the data logged on a 1.2-arcmin grid. The scans extended well beyond the region studied in this paper and covered all of the Vela SNR (as seen in the radio map of Day et al. 1972) either in right ascension, $08^h\ 20^m$ to 09^h (1950), or declination, $-41°30'$ to $-47°30'$. Here I show only the bright Vela X region, since the remainder of the Vela SNR was scanned only in one coordinate. The complete shell of

the Vela SNR can just be seen as a very faint plateau in these longer scans.

3 RESULTS

The 8.4-GHz total-intensity contours and polarization E vectors (at 3-arcmin resolution) are shown in Figs 1 and 2, and in both of these we see a filamentary structure. These filaments are more obvious in Fig. 2(b), which shows the polarization intensity in grey-scale. The bright, isolated point source in the north-east corner of the total-intensity maps is apparently unpolarized. There is no positional agreement between these radio filaments and those seen optically, unlike the radio filaments seen in SNR IC 443 (Dickel et al. 1989).

The total-intensity and polarization maps were then convolved to 4.4 arcmin and to 8.4 arcmin for comparison with the 5- and 2.7-GHz data, respectively, of Paper I. From these comparisons I have derived the distribution of radio spectra, the Faraday rotation measure (RM), the direction of the projected magnetic field, and the depolarization ratio.

The percentage polarization is shown in Fig. 3; the grey-scale represents the polarization degree at full 3-arcmin resolution, and the contours display this same distribution smoothed to 4.4 arcmin to match fig. 9 of Paper I (5-GHz percentage polarization). At full resolution the percentage polarization is greater than 40 per cent in two regions and, in general, the areas of high-percentage polarization follow the polarized filaments of Fig. 2. At 4.4-arcmin resolution the similarity between the contours of percentage polarization at 8.4 GHz and at 5 GHz (Paper I) is clear, and leads to the generally low value of depolarization discussed below.

The radio spectrum. The total-intensity flux density obtained by integrating Fig. 1 is 490 ± 80 Jy (Table 1) and, when compared with the flux densities at 2.7 and 5 GHz obtained for the Vela X component in Paper I, and allowing about ± 10 per cent errors, would admit spectral indices of between -0.4 and -0.8. This large range reflects the relatively short frequency baseline, together with uncertainties about how much of the Vela SNR should be included in the X component as well as the usual uncertainties in base level. Fig. 4 compares the total intensities, and also the polarizations, at both 8.4 and 2.7 GHz; the 8.4-GHz data have been smoothed to 8.4 arcmin, the beamwidth of the 2.7-GHz data taken from fig. 1 of Paper I. The similarity between the two maps is striking and suggests that there is very little variation in the distribution of spectral index (and very little depolarization) over Vela X. The total-intensity spectrum is distributed fairly uniformly over Vela X, exhibits little correlation with other features, and is similar to fig. 4 of Paper I; it is not shown here.

The spectrum of the polarized component between 8.4 and 5 GHz is fairly uniform along the filaments and from filament to filament, with values near -0.4. However, there is a marked variation in spectral index *across* the filaments. This is seen as a steepening of the spectrum along *one* edge (predominantly the outer edge) of each filament. This asymmetry is not thought to be due to resolution differences or to increased noise on the filament edge, both of which would give symmetrical effects across the filaments, nor is it

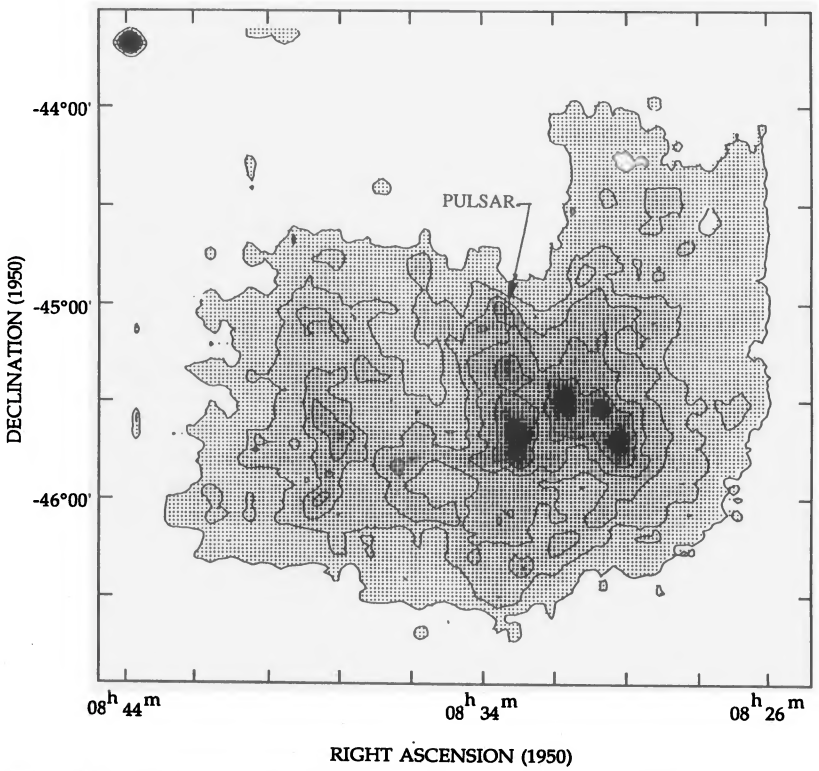

Figure 1. Total-intensity grey-scale and contours of Vela X at 8.4 GHz. The half-power beamwidth is 3.0 arcmin, the contour interval is 90 mJy beam^{-1}, and the position of the Vela pulsar is indicated by a cross.

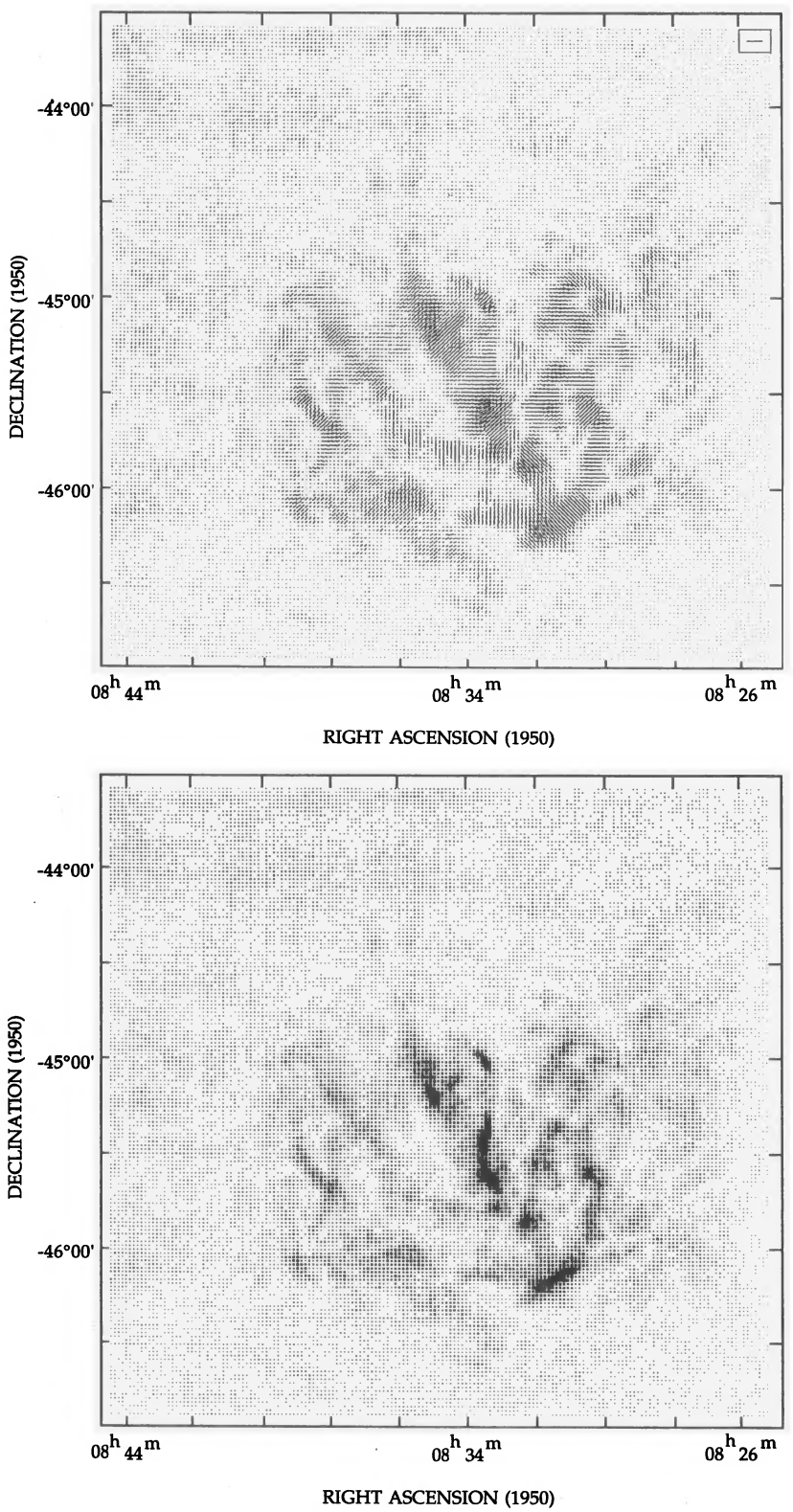

Figure 2. (a) Polarization E vectors and (b) polarization intensity grey-scale of Vela X at 8.4 GHz. The polarization scale is indicated by a 200-mJy beam^{-1} E vector in the inset, the maximum polarization intensity is 146 mJy beam^{-1} and the half-power beamwidth is 3.0 arcmin.

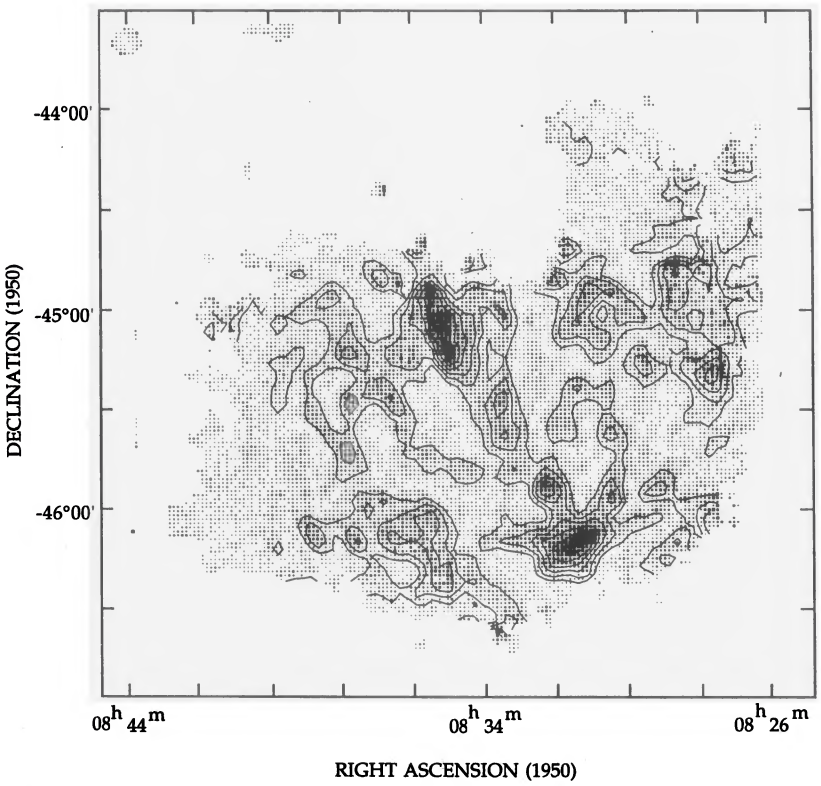

Figure 3. Distribution of degree of polarization over Vela X. The contour interval is 5 per cent linear polarization. The lowest contour is at the 10 per cent level and the highest, 35 per cent level. The contours are smoothed to 4.4-arcmin resolution, and the original 3-arcmin data are shown as a grey-scale.

Table 1. Integrated flux densities for Vela X.

Frequency (MHz)	Flux density (Jy)	Reference
2700	1050	Milne (1980)
5000	759	Milne (1980)
8400	490±80	This paper

likely to be due to poor registration, which would be seen as a steepening always in the same sky direction. The variation in spectral index is reflected in the distribution of depolarization (Fig. 7) with which it would be identical, but the inverse if the total intensities were constant.

Faraday rotation. The distribution of Faraday rotation measure (RM) is shown in Fig. 5. This figure was constructed from the polarization data at 8.4, 5.0 and 2.7 GHz (the last two from Paper I). The resolution is 4.4 arcmin, the resolution of the 5-GHz data, although the lower resolution 2.7-GHz data have also been used. Fig. 5 is limited to those directions where the polarization intensity exceeds 10 per cent of the peak polarization at each frequency used, thus removing most of the more uncertain RM estimates. The RM is positive over most of the field, and the overall mean RM is $+44$ rad m^{-2}, which is close to previous estimates of $+46$ rad m^{-2} (Milne 1968) and $+56\pm26$ rad m^{-2} (Paper I). The Vela pulsar is located in a small region of fairly uniform RM (~ 42 rad m^{-2}). The overall distribution of RM in Fig. 6 is similar to that shown in fig. 7 of Paper I (which is not entirely unexpected, since certain data are common to both analyses), but the present study is more detailed.

Using data at the three frequencies (8.4, 5.0 and 2.7 GHz), I tried to detect non-linearity in RM, which could indicate the presence of *internal* Faraday rotation. For most directions the departures from linearity are slight and well within the probable errors in position angle. However, the curvature is of the same sign and fairly uniform in value over several areas, which would not be expected from purely random errors. Moreover, these areas do not always have the same sign in curvature, which would be expected if there is a systematic offset in the position angle at one frequency. This work is not yet complete; it needs a fourth frequency to be more certain of whether the non-linearity of the RM is real.

The direction of the projected magnetic field deduced from the 8.4-, 5.0- and 2.7-GHz polarization is shown in Fig. 6. This figure has also been constructed at 4.4-arcmin resolution; the 'vector' magnitude is the geometric mean of the available polarization intensities at each point and indicates the reliability of the direction at that point. Fig. 6 shows the magnetic-field directions to be well aligned *along* the polarized filaments prominent in Fig. 2.

The 8.4-/5.0-GHz depolarization ratio (=percentage polarization at 8.4 GHz/percentage polarization at 5 GHz) is shown in Fig. 7; the data are limited to those regions of Vela X where the total intensity is greater than 10 per cent of the peak value. Apart from the presence of high depolarization in regions of lowest polarization intensity, to be expected from errors alone, and the similarity to the polarized spectral

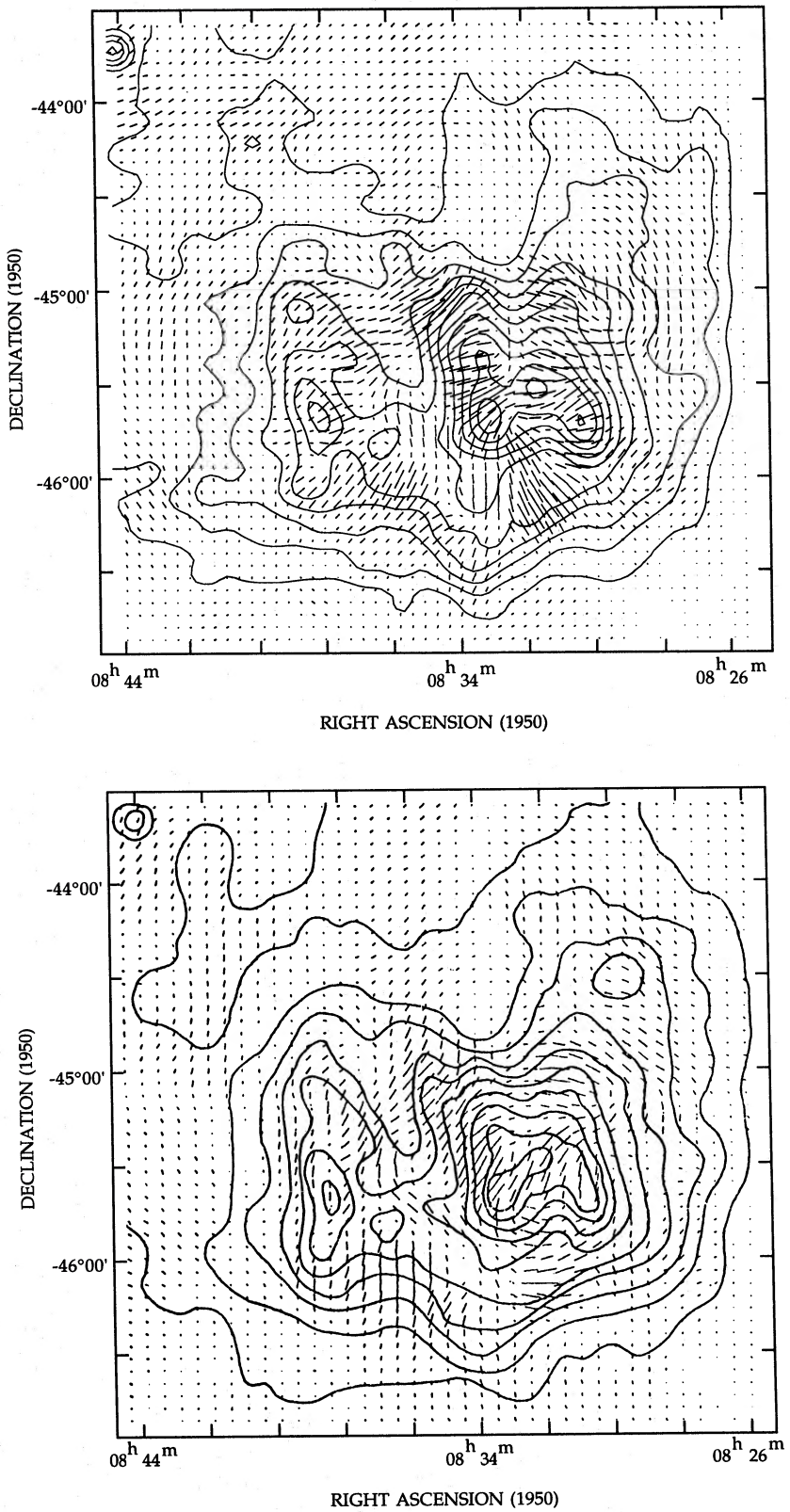

Figure 4. Comparison between (a) 8.4- and (b) 2.7-GHz total-intensity contours and polarization E vectors. The 8.4-GHz data have been smoothed to the resolution of the 2.7-GHz data (8.4 arcmin). The contour intervals are 372 mJy beam^{-1} and 0.5-K full beam brightness temperature at 8.4 and 2.7 GHz, respectively. The 2.7-GHz data are from Paper I, fig. 1.

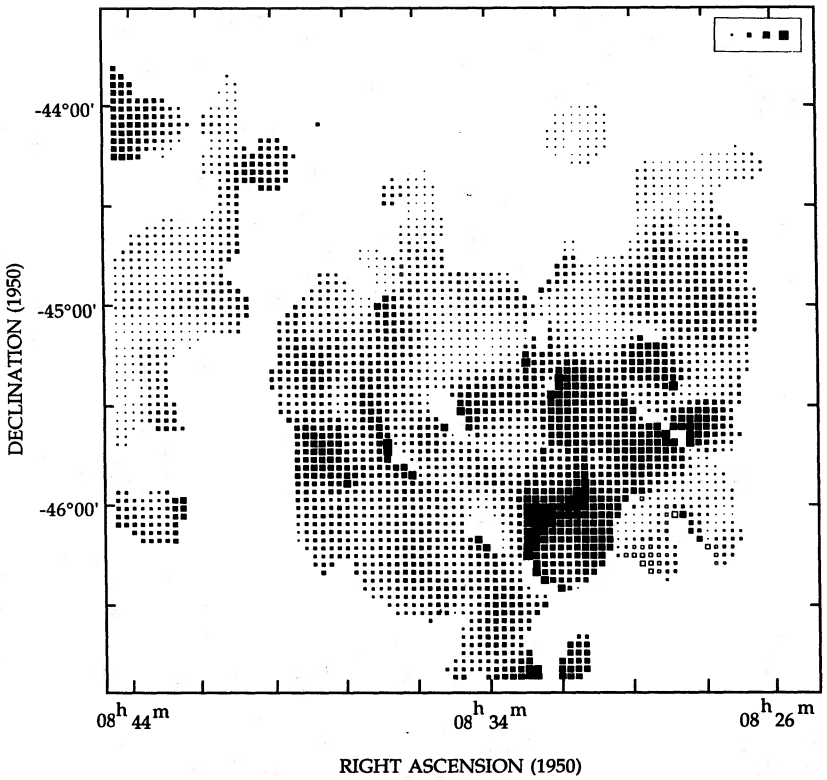

Figure 5. Distribution of rotation measure (RM) over Vela X between 5 and 8.4 GHz. The filled/unfilled boxes indicate positive/negative RM, respectively, while the box size is a measure of the magnitude of the RM at that point. RMs of 20, 60, 100 and 140 rad m^{-2} are indicated in the inset. Values are displayed only where the polarization intensity is > 10 per cent of the peak polarization at both frequencies. The resolution of this figure, and Figs 6 and 7, is 4.4 arcmin, the resolution of the 5-GHz data.

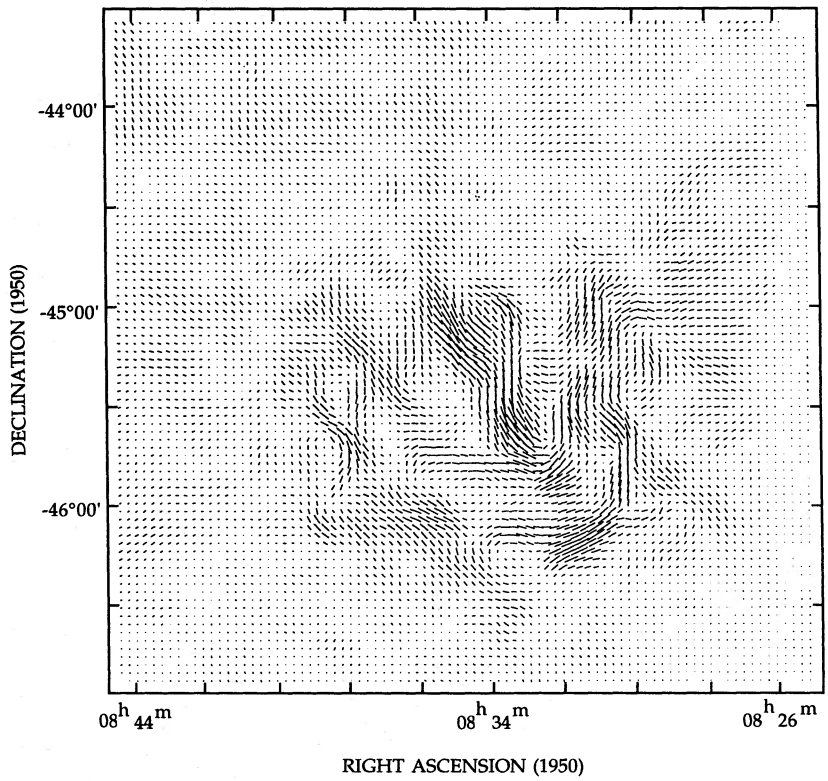

Figure 6. Direction of the projected magnetic field over Vela X. The 'vector' magnitude is proportional to the mean value of the polarization at 8.4, 5 and 2.7 GHz, and provides an indication of the reliability of the field direction at that point.

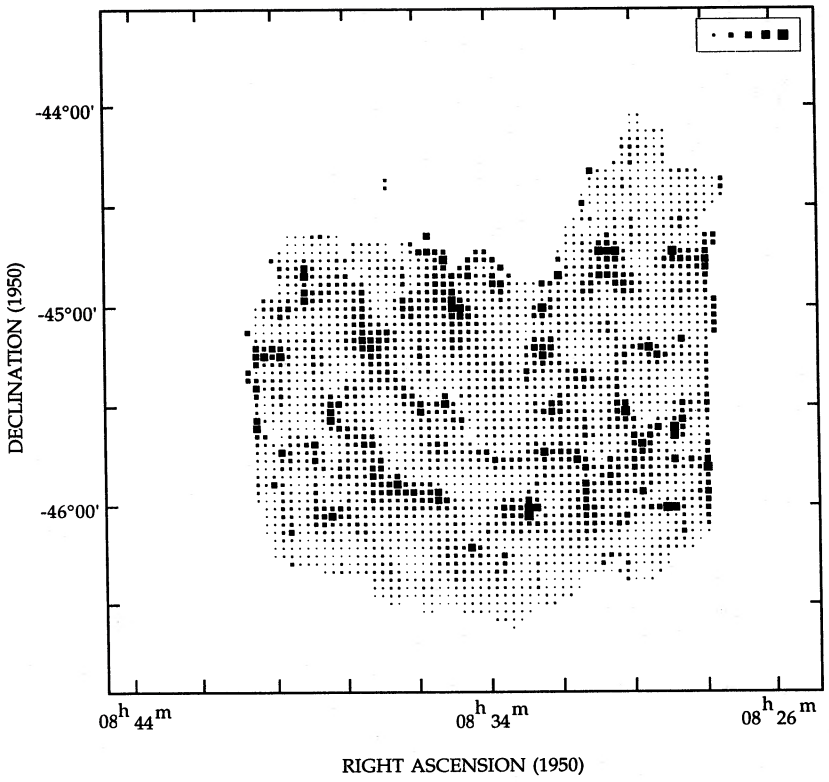

Figure 7. Depolarization ratio (i.e. $P_{8.4\,\mathrm{GHz}}/P_{5\,\mathrm{GHz}}$) over Vela X. Depolarization ratios of 1, 2, 3, 4 and 5 are indicated in the inset. Data are shown only where the total intensity at both frequencies is greater than 10 per cent of the peak intensity.

distribution remarked on above, there is no obvious correlation between the depolarization and any other parameter. In particular, there seems to be no relationship between depolarization and RM gradient as was suggested in Paper I. There are several directions for which the depolarization ratio is less than unity – physically unacceptable values. However, like the high values of depolarization, these are located in regions (often adjacent to regions of high depolarization) where there is little polarization and are most likely not real. Away from these high values, the mean value of the depolarization ratio is 1.1. This was further tested at lower resolution, but with greater confidence, by obtaining the distribution of 8.4-/2.7-GHz depolarization ratio. This was more uniform than over the smaller frequency interval, but did reflect the extremes of Fig. 7. As before, the average value of depolarization ratio is near unity. From this and the remarkable similarity between the 8.4- and 2.7-GHz maps (Fig. 4), I suggest that there is little depolarization over Vela X, except along the outer edges of the filaments.

Filament width. Rosso & Pelletier (1993) show that filament width should depend only on the magnetic field. So, following Velusamy, Roshi & Venugopal (1992), the 8.4-GHz polarization map (Fig. 2b) was smoothed to 20 arcmin and subtracted from Fig. 2(b) to display the narrow polarization features. 25 filament widths were then measured, yielding a mean deconvolved width of 2.5 ± 1.9 arcmin, or 0.34 ± 0.29 pc at a distance of 500 pc (the suggested distance to Vela X). From Rosso & Pelletier's fig. 1, this leads to an estimated magnetic field of between 10^{-5} and 5×10^{-5} G, a totally expected result typical of SNRs and embracing the value for SN1006 (3×10^{-5} G) suggested by Wilson, Samarasinha & Hogg (1989). However, these filaments are barely resolved in the 3-arcmin beam, and high-resolution imaging of selected filaments should be undertaken with either the VLA or the Australia Telescope Compact Array (ATCA).

4 DISCUSSION

At 8.4 GHz, 3.0-arcmin resolution, Vela X appears as a bright region on a very low-surface-brightness plateau, which makes it difficult to assess the spectral index. However, comparison of the present image (at 8.4 GHz) with that at 2.7 GHz suggests to me that the spectral index is remarkably constant (with a value between -0.4 and -0.8) at least over the brighter parts of the SNR. While variation in spectral index over the remnant has been used to argue that the Vela SNR consists of two separate remnants, it now appears from the *ROSAT* image that the Vela SNR is one remnant with the pulsar at its centre.

The remnant is strongly polarized, >40 per cent at 8.4 GHz, and exhibits very little or no depolarization. Faraday rotation is relatively low (~ 44 rad m^{-2}), reasonably uniform and close to values obtained previously. The RM in the direction of the Vela pulsar is 42 rad m^{-2}.

Most important perhaps in this investigation is the discovery that much of the radio emission appears as polarized filaments, with the magnetic field directed along these filaments, a feature previously seen only in the Crab Nebula (Velusamy et al. 1992). These radio filaments are apparently

unrelated to the optical or X-ray features, such as those seen in IC 443 where the radio and optical features are coincident and presumably both due to the same mechanism – shock heating and evaporative cooling of overrun interstellar clouds (Dickel et al. 1989). Furthermore, the magnetic field in the IC 443 filaments is skewed across the filaments, consistent with the passage of an oblique shock (Wood, Mufson & Dickel 1991).

In the Crab Nebula there is good agreement between the optical (line-emitting) and radio filaments in the central region, but the outer regions contain a number of distinct radio loops and arches with no optical counterpart. Also, similar to Vela X, the magnetic field is directed *along* these filaments (Velusamy et al. 1992). These authors suggest that the toroidal nebular magnetic field is compressed and frozen into the filamentary structures and then stretched into loops and arches. They also find a marked steepening of the filamentary spectral index with increasing distance from the pulsar – an effect that we do not see in Vela X.

While searching for spectral effects in the filament polarization, I noted that the spectrum was steeper on one edge of each filament. This is also reflected in the depolarization distribution and, if genuine, may be either an intrinsic spectral effect, presumably due to a steepening of the electron distribution at the outer face of a 'sheet-on-edge' filament, or to depolarization (perhaps a more acceptable model if the filaments are to be considered as tubes). In the latter case, however, it is hard to imagine why the depolarization should be on one side of the filament only.

Separating the filaments from the broad structure by high-pass filtering, and subsequently measuring them, yielded observed sizes of typically 3 to 4 arcmin, unfortunately close to the resolution of the telescope. Moreover, while the deconvolved diameters are in the broad size range predicted by Rosso & Pelletier (1993), high-resolution imaging with either the VLA or the ATCA should be done to resolve these filaments more clearly.

The 'jet' recently discovered by Markowardt & Ögelman (1995) does have a radio counterpart in the bright filament extending south from the pulsar for 45 arcmin. It is distinctive in that, even though it is one of the brightest features in polarized intensity (Fig. 3), it does not have a high degree of polarization (~ 15 to 20 per cent in Fig. 4). The absence of evidence for depolarization or a tangled magnetic field suggests that it may have a high thermal content, in agreement with the suggested thermal nature of the X-ray jet.

Reynolds (1988) has reviewed the possible explanation for filaments in SNRs and concludes that a pulsar-generated magnetic flux and relativistic particles interacting with the thermal filamentary structures, caused by the Rayleigh–Taylor instability operating on thermal gas accelerated by the pulsar, is the most likely model. A strong thermal contribution is needed in Reynold's model, which could be seen as a variation in the radio spectra of the filaments. High-resolution studies with the ATCA, planned for mid-1995, may answer some of the questions raised in this paper.

REFERENCES

Aschenbach B., Egger R., Trümper J., 1995, Nat, 373, 587
Day G. A., Caswell J. L., Cooke D. J., 1972, Aust. J. Phys. Astrophys. Suppl. No. 25
Dickel J. D., Williamson C. E., Mufson S. L., Wood C. A., 1989, AJ, 98, 1363
Dwarakanath K. S., 1991, J. Astrophys. Astron., 12, 199
Kahn S. M., Gorenstein P., Harnden F. R., Seward F. D., 1985, ApJ, 299, 821
Markwardt C. B., Ögelman H., 1995, Nat, 375, 40
Miller E. W., 1973, PASP, 85, 764
Milne D. K., 1968, Aust. J. Phys., 21, 201
Milne D. K., 1980, A&A, 81, 293 (Paper I)
Milne D. K., Manchester R. N., 1986, A&A, 167, 117
Reynolds S. P., 1988, ApJ, 327, 853
Rosso F., Pelletier G., 1993, A&A, 270, 416
Tabara H., Inoue M., 1980, A&AS, 39, 379
Velusamy T., Roshi D., Venugopal V. R., 1992, MNRAS, 255, 210
Wilson A. S., Samarasinha N. H., Hogg D. E., 1989, in The Crab Nebula and Related Supernova Remnants. Cambridge Univ. Press, Cambridge, p. 139
Wood C. A., Mufson S. L., Dickel J. R., 1991, AJ, 102, 224
Wright A. E., Otrupcek R. E., 1990, PKSCAT90: The Southern Radio Sources Database V1.01. Sydney, Australia Telescope National Facility, CSIRO